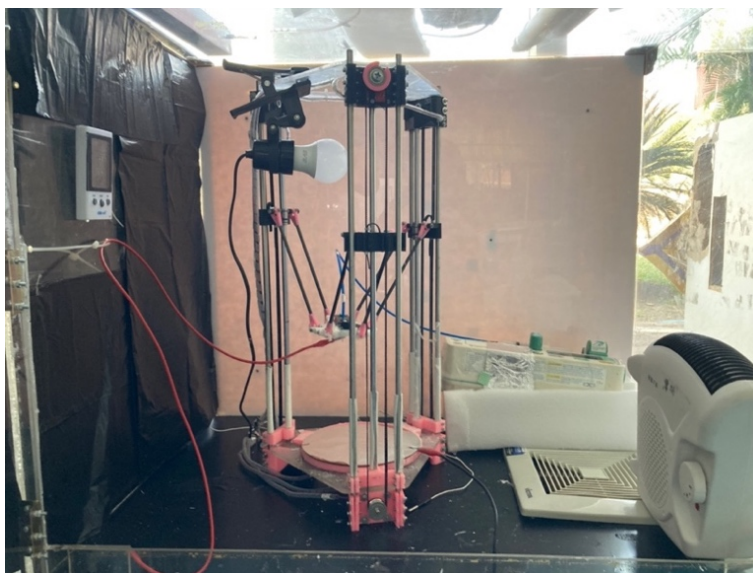# CHAPTER V

CONCLUSION

The objectives, hypotheses, and basic principles, outlined in Chapters I and II, were amalgamated with an extensive assortment of 3D electrospinning assembly and characterizations in Chapter III, which focused on the assembly of 3D electrospinning and characterization of 3D fibrous macrostructures and biological activities. Chapter IV, specifically section 4.1, discussed the proper setup for 3D electrospinning. Additionally, it explored the conditions and characteristics necessary to produce self-assembled electrospun stacks and build 3D fibrous macrostructures, as discussed in section 4.2 of Chapter IV. Furthermore, the biocompatibilities of the 3D fibrous constructions were evaluated through *in vitro* cell culture using SEM, SR-FTIR and SRXTM techniques in section 4.3 of Chapter IV.

As stated in hypothesis I, the investigation focused on the 3D electrospinning technique using cartesian and delta coordinates. It was discovered that both coordinates face the common issue of fibers being deposited in undesirable locations. Nevertheless, the delta framework effectively avoided this issue by incorporating silicon onto the tower in areas outside of the reach of the carriages. Here, the delta coordinate was used to be the mechanical component of 3D electrospinning. Figure 5.1 showcases the most recent version of 3D electrospinning. This device allows for the buildup and control of 3D fibrous macrostructures. It has a maximum printing area of 500 mm in height and 180 mm in diameter. The flow rate can range from 0.1 to 300 ml/h, and a voltage source can be applied in a range from 1.0 to 50.0 kV.

Figure 5.1 The current version of 3D electrospinning setup in this work.

The results from Chapter 4, particularly in section 4.2 (as seen in Figure 5.2), provide confirmation that supports hypothesis II in this study. The conductivity of a solution is a significant component to facilitating the self-assembly of 3D fibrous structures. The addition of H3PO4 additives was crucial for the 3D electrospun stack of PCL and PVDF, but the PAN solution in DMF solvent did not require the additives. The addition of H3PO4 additives did not change the chemical bonding and crystalline structures of PCL and PVDF, as indicated in the XRD pattern, FTIR spectra, and Raman spectra. However, the process of electrospinning caused a phase change in PVDF by increasing the β phase on the electrospun fiber, as confirmed by the XRD pattern.

Undoubtedly, the addition of H_3PO_4 in a solution provides greater potential for constructing 3D fibrous macrostructures. Nevertheless, the high presence of H_3PO_4 leads to the formation of bead-like fibers and fluffy fibrous structures, making it challenging to precisely regulate the positioning of the incoming fiber during deposition. The formation of 3D fibrous macrostructures is influenced not only by conductivity but also by the concentration, which determines the number of incoming fibers. The concentration may not have an apparent impact when the nozzle is fixed, but it is essential when the nozzle is in motion. If the concentration is insufficient, the fiber being produced will not be continuous and the distance between the nozzle and the collector will progressively increase, resulting in spatial

dispersion in two dimensions. The increased concentration causes the solution at the nozzle tip to dry out and can potentially impact vertical structures due to the weight of a large amount of fiber. Furthermore, it is crucial to ensure that the solvent is properly proportioned with the concentration and flow rate in order to achieve sufficient evaporation during electrospinning, under the specified conditions. The flow rate factor provides results that closely correspond to the concentration. The building of 3D electrospun macrostructures is influenced not only by the flow rate and concentration, but also by other parameters such as initial distance, voltage, and moving speed. The insufficient starting distance hinders the development of three-dimensional macrostructures, whereas an excessive initial distance results in the construction of a two-dimensional mat instead of a three-dimensional stack. The effect of solution and electrospinning on 3D fibrous macrostructures are concluded in Table 5.1 based on the empirical tests.

Table 5.1 The effect of electrospinning parameters on the shape of 3D macrostructures.

Parameters	Height	C_{hh}	DW	D_{out}	Wall thickness	Diameter
↑ Flow rate	≈	↑	↑↓	↓	↓	≈
↑ Initial Distance	≈	↑	↑ *	↑	↑	↑*
↑ Voltage	↑↓	↑↓	↓	↓	↓	↓
↑ Nozzle's Speed	↑↓	↑	↑	-	↑	↑

Note ↑ = increase, ↓ = decrease, ≈ = fluctuation, ↑↓ = increase until the point and then decreases, * = based on the separation of consideration between 2D mat and 3D structures.
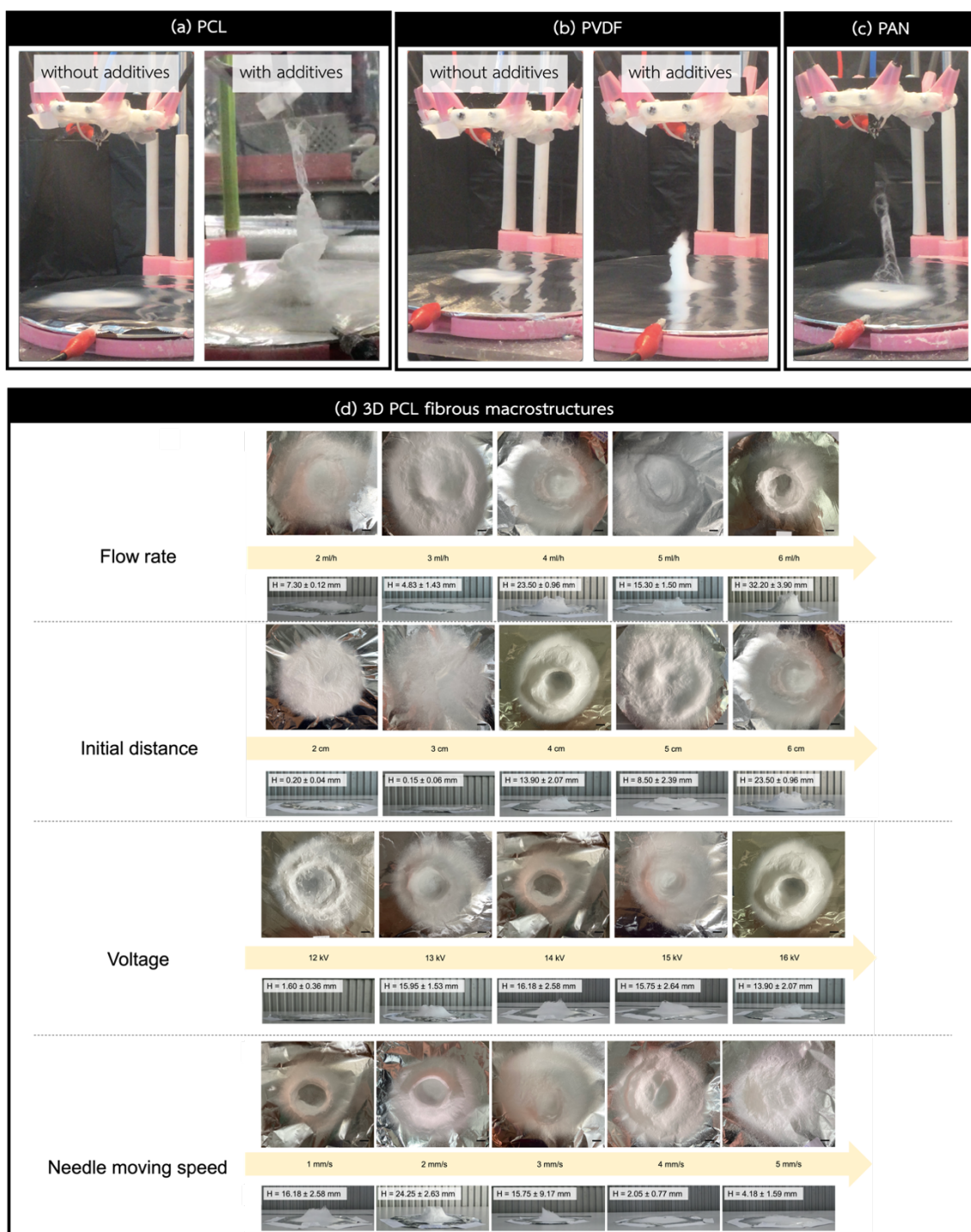
Figure 5.2 Photographs of 2D mat and 3D stack electrospun (a) using PCL solution without and with the H_3PO_4 additives, (b) using PVDF solution without and with the H_3PO_4 additives, (c) 3D stack using PAN solution, and (d) the influence of electrospinning parameters on the 3D fibrous macrostructures.

The results presented in Section 4.3 of Chapter 4 provide support for Hypotheses III and IV of this work. The hydrophilic property of 3D PCL fibrous structures can be enhanced via plasma treatment, which is essential for cell culture. The optimal conditions of plasma treatment yield favorable results in *in vitro* cell culture. If the power applied in the plasma treatment was low, the hydrophilic property underwent modifications. Conversely, if excessively high power was given, it resulted in the melting and a lack of fibers, both of which were not favor to cell adhesion. In part of biological assessment, the SR-FTIR imaging techniques can provide the mapping used to track the location of cell on the fibrous sample. Furthermore, the analytical method of SR-FTIR imaging with HCA is able to provide distribution information. In this work, the results of SR-FTIR imaging with HCA implied the content of 5 wt% cullulose performed the most uniform distribution of cells on the fiber as shown in Table 4.6. The SRXTM technique is a potential tool for observing the cell morphology and adhesion within 3D PCL scaffolds. Not only the observation on the surface of electrospun graft, but also the inside of graft can be observed, as seen in Figure 5.3. In addition, the normalized volume of cell by compared to the volume of fiber can imply to the cell growth inside the electrospun graft.

As an aspect of biological assessments, the SR-FTIR imaging techniques can be utilized to generate a map that accurately traces the position of cells on the fibrous sample and assess the distribution of components. The analytical method of SR-FTIR imaging can provide quantitative results, allowing for comparable outcomes to reach the optimal condition. It is an effective technique for observing and analyzing the biochemical composition. It can not only indicate the distribution of components but also accurately monitor the location of composites. Furthermore, the SRXTM approach has the potential to be used as a tool for monitoring the cell morphology and adhesion within 3D PCL scaffolds. The top view, cross section, and bottom view of the electrospun graft can be viewed, as depicted in Figure 5.3. Furthermore, the volume of cell can indicate existing cell growth within the electrospun graft. When comparing the volume of cells cultivated for 1 and 3 days, the ratio of the

NIH3T3 cell's normalized volume to the volume of the PCL graft in this work can indicate a double rise in NIH3T3 cell growth within the PCL electrospun graft.
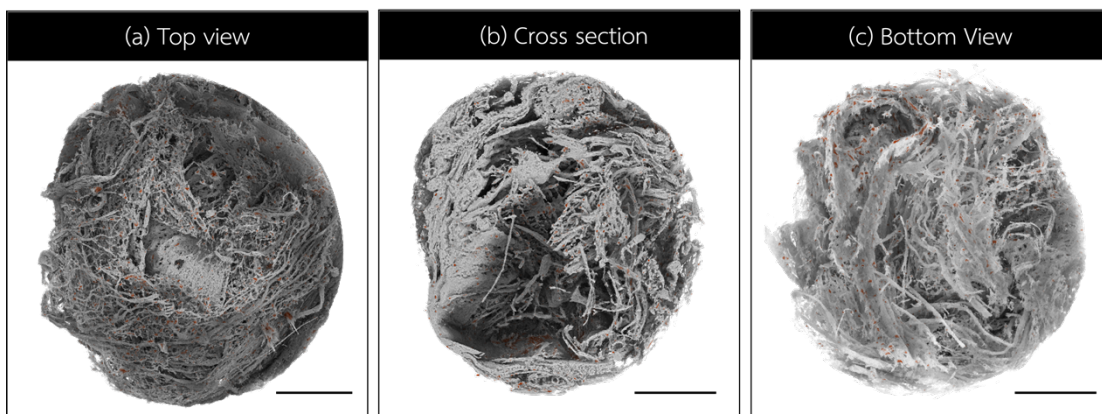
Figure 5.3 SRXTM images of NIH3T3 cells (shown by red spots) cultivated on PCL fiber structures (represented by gray region). The imaging was performed from (a) the top view, (b) cross section, and (c) bottom view. The scale bar is 500 um.

Future Perspectives

The conclusions of this work demonstrate the capacity of 3D electrospinning to create 3D fibrous macrostructures, as well as the efficiency of the SR-FTIR and SRXTM approaches for biological evaluations. The results show that it is feasible to gather electrospun fibers during the early whipping phase in order to construct 3D electrospun macrostructures. Further, the resulting 3D macrostructures possess biocompatible abilities following the proper improvement. As stated in the expected impact outlined in section 1.5 of Chapter I, next prospects will integrate the tests, parameters, and modeling through the utilization of 3D electrospinning to produce more polymers and composites. The number of 3D self-assembled structures achieved using 3D electrospinning has the potential to significantly increase. The utilization of SR-FTIR and SRXTM techniques for observing biological activity is expected to expand and develop.

This advancement in 3D electrospinning not only overcomes current constraints in scaffold fabrication but also opens up possibilities for groundbreaking applications in various fields. The precise design and enhanced capabilities of these

large-scale structures have considerable potential for expanding the field of lab-grown organs and creating artificial tissues. Furthermore, the foundational work laid by this 3D electrospinning method sets the stage for advancements in 4D printing, particularly in the development of dynamic, responsive fibrous materials, opening new horizons in biomedical engineering and beyond.